Strength Dependence of Cadherin-Mediated Adhesions

Benoit Ladoux,[†‡*] Ester Anon,[†] Mireille Lambert,[§‖] Aleksandr Rabodzey,[†] Pascal Hersen,[†] Axel Buguin,[¶‖] Pascal Silberzan,[¶] and René-Marc Mège[§‖*]

[†]Laboratoire Matière et Systèmes Complexes, Centre National de la Recherche Scientifique, Unite Mixte de Recherche 7057, Université Paris Diderot, Paris, France; [‡]Research Center of Excellence in Mechanobiology, National University of Singapore, Singapore; [§]Institut National de la Santé et de la Recherche Médicale, U839, Institut du Fer à Moulin, Paris, France; [¶]Laboratoire Physico-Chimie Curie, Centre National de la Recherche Scientifique, Unite Mixte de Recherche 168, Institut Curie, Paris, France; and [‖]Université Pierre et Marie Curie-Paris 6, Paris, France

ABSTRACT Traction forces between adhesive cells play an important role in a number of collective cell processes. Intercellular contacts, in particular cadherin-based intercellular junctions, are the major means of transmitting force within tissues. We investigated the effect of cellular tension on the formation of cadherin-cadherin contacts by spreading cells on substrates with tunable stiffness coated with N-cadherin homophilic ligands. On the most rigid substrates, cells appear well-spread and present cadherin adhesions and cytoskeletal organization similar to those classically observed on cadherin-coated glass substrates. However, when cells are cultured on softer substrates, a change in morphology is observed: the cells are less spread, with a more disorganized actin network. A quantitative analysis of the cells adhering on the cadherin-coated surfaces shows that forces are correlated with the formation of cadherin adhesions. The stiffer the substrates, the larger are the average traction forces and the more developed are the cadherin adhesions. When cells are treated with blebbistatin to inhibit myosin II, the forces decrease and the cadherin adhesions disappear. Together, these findings are consistent with a mechanosensitive regulation of cadherin-mediated intercellular junctions through the cellular contractile machinery.

INTRODUCTION

Cell adhesion plays an important role in the regulation of many physiological and pathological processes. Living cells are able to sense their environment and adequately respond in terms of morphology, migration, proliferation, differentiation, and survival (1). For instance, embryonic development involves a specific and complex architectural organization of biological tissues. Embryonic cells adhere, migrate, segregate, and differentiate in a selective and coordinated fashion. Further steps include the formation of specific cellular junctions that contribute to the mechanical cohesion of tissues and allow cell communication. Thus, it is important to understand how, according to their physiological state and position in the embryo or tissue, cells can establish and regulate precise contacts with adjacent cells (2). It is also essential to understand how cells can interpret ''contact'' information and transmit chemical and mechanical signals to the cytoskeleton, the cytoplasm, and the nucleus to allow an adapted cellular response. In this context, one of the important features of the adhesion of cells is their mechanical interaction with the external environment and their ability to develop forces at adhesion sites (3).

Several families of cell surface glycoproteins have been characterized, including IgCAMs, cadherins, and integrins, which are responsible for specific cell-cell and cell-matrix adhesion. Such receptors, which are physically or functionally linked to the cytoskeleton through specific cytoplasmic adaptors, are ideal candidates for mediating mechanochemical signal transduction. The traction forces developed and transmitted via integrins by cells toward the extracellular matrix (ECM) were first proposed more than a decade ago and recently characterized in detail (4–7). In particular, ECM rigidity and external forces appear to be key parameters affecting mechanical stress and cell tension (1,8–11), and thus significantly influence cell functions (12–14). Intercellular forces play a critical role in a number of collective cell processes, such as cell rearrangement/tissue reshaping during normal embryonic morphogenesis (15–17), and physiopathological situations such as cancer development (18–20) and scar tissue formation. They may also be important for leukocyte transmigration and inflammatory processes (21,22), and cell differentiation (23). Cadherins are of special interest as regards force transmission through cell-cell junctions because they constitute a universal family in the animal kingdom, i.e., all members act as both their own ligands and receptors in cell-cell contacts, and establish a direct link between the adjacent cell and the cytoskeleton (17).

To date, the transmission of forces through cadherin-based intercellular junctions has not been studied to the same extent at the cellular level, partly due to the lack of methods combining the detection of nanonewton-level forces and a molecular control of cell-cell interactions (24). Various experiments have been used to measure the interaction strength of cadherins at the molecular level, using such techniques as hydrodynamic flow (25), AFM cantilevers (26) in the surface force apparatus (27,28), and microbeads in the biomembrane force probe (29,30). These methods can assess

Submitted July 14, 2009, and accepted for publication October 29, 2009.

*Correspondence: benoit.ladoux@univ-paris-diderot.fr or Rene-Marc.Mege@inserm.fr

Mireille Lambert's present address is Département d'Hématologie-Immunologie, INSERM U567, Institut Cochin, Paris, France.

Editor: Denis Wirtz.

0006-3495/10/02/0534/9 $2.00

doi: 10.1016/j.bpj.2009.10.044

the function and attachment force of individual cadherin ectodomains, but they cannot account for the integration of inside-out and outside-in signaling (31). On the other hand, estimating the force mediated by cadherins between suspended cells in a dual-pipette assay (32) does not allow access to subcellular details. Recent studies have examined the strengthening of cadherin-mediated intercellular adhesion between living cells using single-molecule force spectroscopy over short timescales, and the results suggest that cadherin bonds form cooperatively, independently of actin cytoskeleton (33,34). Since the adhesive engagement of cadherins triggers their anchoring to the contractile actomyosin network (35–38), cells may experience local variable tension from their neighbors over time and locally adapt the composition of the adhesion complexes and cytoskeleton to balance external and internal mechanical loads (39). Therefore, it is crucial to study the influence of tunable external tension on intercellular contact formation and cellular tensile forces. On the basis of previous rigidity-sensing studies at the cell-ECM interface (8,12), we varied the mechanical environment to study the effect of mechanical forces and cellular tension on the formation of cadherin junctions.

MATERIALS AND METHODS

Fabrication and calibration of the substrates

Polyacrylamide (PA) gel samples were prepared on aminosilanized glass coverslips according to published methods (9). Briefly, to control or adjust the gel's stiffness, the cross-linker *n,n′*-methylene-bisacrylamide was mixed with acrylamide;~50 μL of the mixture were reticulated on a coverslip using a 1/200 volume of 10% ammonium persulfate and 1/2000 volume of *n,n,n′,n′*-tetramethylethylenediamine. The polymerizing gel was covered with a second coverslip pretreated with dichlorodimethylsilane to ensure easy detachment and a uniform polymerized gel surface. The final gels were ~100 μm thick as measured by microscopy. Anti-human Fcγ fragment antibodies (Jackson ImmunoResearch, West Grove, PA) were chemically cross-linked using a photoactivating cross-linker, sulfo-SANPAH (Pierce, Rockford, IL), to the surface of the gels. The substrates were then incubated overnight with purified N-cadherin Ncad-Fc chimera (40).

Polydimethylsiloxane (PDMS) micropillar arrays were prepared as described previously (41). Briefly, using conventional photolithography followed by a deep etching process (the "Bosch process"), silicon wafers were patterned with an array of cylindrical pits, and the desired pattern was replicated in positive photoresist by photolithography. The bare parts of the wafers were then etched by the deep silicon etching process down to the desired depth to obtain the negative pattern of the array. A drop of liquid silicone (PDMS, Sylgard 184; Dow Corning, Midland, MI), was placed on the silicon template between two zero-thickness coverslips (0.08–0.13 mm) and covered by another coverslip to obtain a 0.08–0.13-mm-thick microchip, cured at 65°C for 12 h, and peeled off in 70% ethanol to prevent collapse of the pillars. The ethanol was then gradually replaced by phosphate-buffered saline (PBS). Pillars of the same areal density (22%; ratio of the post surface to the total surface) were used in all experiments with a pillar diameter of 2 μm and center-to center distance of 4 μm. To change the rigidity, the pillar height was varied from 3 to 6.5 μm.

We determined substrate stiffness using two methods. To evaluate the Young's modulus of both materials, we used dimensionally calibrated macroscopic cylinders of the materials ($l = 4$ cm in height and 2 cm in diameter) and measured their compressions under a fixed normal strain, σ. The Young's modulus, E, was calculated according to the equation $E = \sigma(\Delta l/l)$, where Δl is the change in length. For the PDMS, we obtained a Young's modulus of 2 MPa $\pm$ 0.1 MPa. In addition, we used calibrated glass microplates to directly evaluate the spring constant of the pillars as previously described (41). The plates were mounted onto a piezoelectric manipulator fixed on the microscope stage. The top of an individual pillar was placed in contact with the microplate displaced by the piezomanipulator, and the deflection of the post was measured by videomicroscopy. We used this method to directly measure the spring constant of PDMS micropillars or to obtain an additional measurement of the Young's modulus, E, of PA gels by fabricating micropillar substrates in PA gels (42). Both methods gave similar results.

Microprinting the substrates on PDMS surfaces

The silicone micropillar arrays were coated with a chicken Ncad-human Fc chimera (40) and a Texas Red fluorescent antibody to visualize the pillars. A 1-mm-thin layer of PDMS (~1 cm $\times$ 1 cm) was treated with air plasma (plasma cleaner; Harrick Scientific, Ithaca, NY) for 1 min and silanized under vacuum with tridecafluoro-trichlorosilane. A 100 μL drop containing 5 μg of anti-human IgG antibodies (Jackson ImmunoResearch Laboratories) in borate buffer 0.1 M, pH 8, was deposited on the silanized PDMS substrate, gently pressed against the entire surface with a glass coverslip, and left to adsorb overnight at 4°C. The array was then rinsed three times with PBS. Then a 100 μL PBS drop containing 10 μg of Ncad-Fc chimera mixed with 0.1 μL Texas Red-conjugated antibody was deposited on the silanized substrate, gently pressed against the entire surface with a glass coverslip, and left to bind for 1–2 h at room temperature. By this method, we delivered Ncad-Fe onto the tips of the posts (43). We then adsorbed bovine serum albumin (BSA) and Pluronics (PBS buffer solution containing 3% BSA, 0.1% Pluronics (F127) for 1 h) onto the remaining unstamped regions of the array to block nonspecific protein adsorption and cell adhesion (6), followed by rinsing with PBS.

Cell culture and blebbistatin and cytochalasin D treatments

C2 mouse myogenic cells were cultured in Dulbecco's modified Eagle's medium (DMEM) containing 10% fetal calf serum at 37°C in 7.5% CO_2. Before each experiment, the cells were mechanically detached from the culture flask in the presence of PBS, 3.5 mM EDTA, 2% BSA. The cells were resuspended in DMEM, deposited on functionalized arrays, and placed in the incubator for 2 h at 37°C in the absence of serum. For control experiments, cells were incubated with a peptide (Peptide2000; Integra Lifescience) containing the arginine-glycine-aspartic tripeptide (RGD) sequence at a 0.5 mg/mL concentration (44). Cells were pretreated with either blebbistatin (Calbiochem) or cytochalasin D (Sigma) at 50 μM for 20 min and 2 μg/mL for 10 min, respectively. The treatment was maintained during the experiment.

Immunofluorescent staining

Cells on micropillar substrates were fixed for 10 min at room temperature using 3% formaldehyde, 4% sucrose in PBS. They were then rinsed in PBS and permeabilized for 5 min with 0.5% Triton X-100 in PBS, blocked for 1 h with 3% BSA in PBS, and rinsed again in PBS. They were then incubated for 1 h with rabbit anti-β-catenin primary antibody (Sigma) at 1/500 dilution in PBS-BSA, rinsed, incubated 1 h with anti-mouse TRITC and/or anti-rabbit Alexa 633 conjugated antibodies (Jackson ImmunoResearch Laboratories) at 1/500 dilution, and then rinsed in PBS. The actin cytoskeleton was stained with Alexa 488 phalloidin (Molecular Probes) at 1/1000 dilution, after which the cells were rinsed in PBS. Preparations were mounted in Mowiol, 90% glycerol, PBS. Images were taken with an Olympus IX71 microscope equipped with a 100$\times$ oil objective.

Confocal scanning microscopy

Images were taken with a Leica confocal imaging system (TCS4D) fitted with a 63$\times$ oil immersion objective (N.A. = 1.32). Acquisitions were

done in a sequential mode using excitation beams at 488, 543, and 633 nm corresponding to maximum excitation wavelengths of GFP, TRITC, and Cy5, respectively. Each captured image corresponded to a single optical slice of 0.5 μm on the upper side of the pillars.

Live-cell imaging

Time-lapse microscopy experiments were performed on an inverted Olympus IX71 microscope (equipped with a 100× oil objective and a heating stage to maintain a controlled temperature of 37°C) coupled to a Cascade digital camera (Roper Scientific). Acquisitions were started 3 h after the deposition of cells on the micropillar substrates.

Image analysis, spreading area, and calculation of traction forces

We calculated the average cell area using Image J software. We analyzed 25 cells from two different pillar chips for each rigidity spring constant, and measured the local deformation of the pillars by using in-house-made multiparticle tracking software (41). In fluorescent microscopy, the local contrast between the top of the posts and the background is high enough to allow for a good determination of each post position by using a simple fit. Our spatial resolution on the position of the pillars was ~30 nm.

RESULTS AND DISCUSSION

Cell spreading on Ncad-coated substrates is stiffness-dependent

We previously showed that cadherin-expressing cells respond to glass surfaces coated with cadherins by an extensive spreading and maturation of cadherin adhesion mimicking cell-cell contacts and adherens junction formation, respectively (45). However, a glass substratum is an extremely rigid surface (with a Young's modulus, E, on the order of 100 GPa) that has no biological equivalent in any tissues of the body (1). Therefore, it was interesting to measure the response of cells to cadherin-coated substrates characterized by E-values ranging from ~5 to 150 kPa. Such a range of rigidities corresponds to the different stiffnesses that cells may encounter in their in vivo microenvironment depending on the tissues involved, particularly regarding the connections with their neighbors (13,46).

First, we plated N-cadherin-expressing myogenic C2 cells on flexible PA gels (9) coated with recombinant ligands composed of Ncad ectodomain coupled to a IgG Fc fragment (Ncad-Fc). By adjusting the bisacrylamide/acrylamide ratio, we were able to vary the Young's modulus, E, of the gels between 10 kPa and 95 kPa (hereafter referred to as soft and rigid substrates, respectively). After 2–3 h, the cells plated on rigid substrates exhibited a typical fried-egg morphology characterized by a large circular lamellipodium (Fig. 1 *A*), as previously observed on glass substrates (45). The mean spreading area of the attached cells was 2070 ± 420 μm^2 ($n = 85$; Fig. 1 *C*). By comparison, the cells seeded on soft substrates ($E = 11$ kPa) showed reduced spreading (~350 ± 110 μm^2; $n = 88$) and no lamellipodium extension (Fig. 1, *B* and *C*). On rigid substrates, as observed on glass, Ncad-catenin complexes were recruited at the cell substratum interface and accumulated in radial structures revealed by anti-β-catenin antibodies within the lamellipodium (Fig. 1 *A*). The actin cytoskeleton was characterized by a circular network of filaments surrounding the nucleus together with radial cables directed toward and ending in Ncad-catenin complexes. In contrast, no stress fibers or recruitment of β-catenin into radial structures were detected in C2 cells on softer substrates (Fig. 1 *B*).

To assess cadherin-mediated traction forces as a function of substrate rigidity, we also plated C2 cells on Ncad-coated micropillar substrates made in PDMS elastomer (43). By changing the height of the pillars from 6.5 to 3 μm, we were able to vary the spring constant of the pillars from 8 up to 170 nN/μm while keeping the surface area of micropillars exposed to the cells unchanged, with fixed density and diameter of the pillars. An estimation of the effective Young's modulus, E_{eff}, of such micropillar substrates led to values ranging from ~5 to 125 kPa (8). Cell spreading and cadherin adhesion formation on micropillar substrates were comparable to those obtained on continuous PA gels. We found that cells were more spread on stiff pillars than on soft ones (Fig. 1, *D–I*). The spreading area dropped from 2320 ± 570 ($n = 83$) to 310 ± 150 μm^2 ($n = 87$) for pillar spring constants varying from 120 ($E_{eff} = 86$ kPa) down to 17.2 nN/μm (~13 kPa), respectively, in agreement with our measurements in PA gels of similar stiffnesses (Fig. 1 *C*). Altogether, these observations demonstrate that C2 cells efficiently spread and form extensive cadherin-mediated cell contacts on substrates with a stiffness comparable to what cells encounter in their tissular microenvironment. However, they also indicate that cadherin adhesion formation is highly dependent on the mechanical properties of the environment over a physiologically relevant range of stiffness values.

The formation of cadherin adhesions depends on the external physical environment

Soft substrates did not support the formation of robust actin cables, as revealed by the diffuse F-actin staining (Fig. 1 *H*). They were also unable to support the formation of large cadherin-catenin complexes, as revealed by β-catenin immunostaining (Fig. 1 *G*). To the contrary, more than 50% of the cells exhibited radially oriented actin cables directed toward and ending in β-catenin-positive radial microstructures on stiff substrates (Fig. 1, *D–F*). These radial patterns (i.e., catenin complexes coupled to a well-structured actin network) were never observed on soft pillars. The analysis of the localization of fluorescence signals due to β-catenin and F-actin stainings (Fig. 2, *A* and *B*) indicated that both signals colocalized within the cell edge on stiff and soft substrates. However, on stiff substrates, the fluorescence intensity for both stainings exhibited a large contrast, with a 10-fold increase for the maximal values that correspond to β-catenin radial structures (Fig. 2 *A*), whereas small variations in intensity, by only a factor of 3, were observed on soft substrates

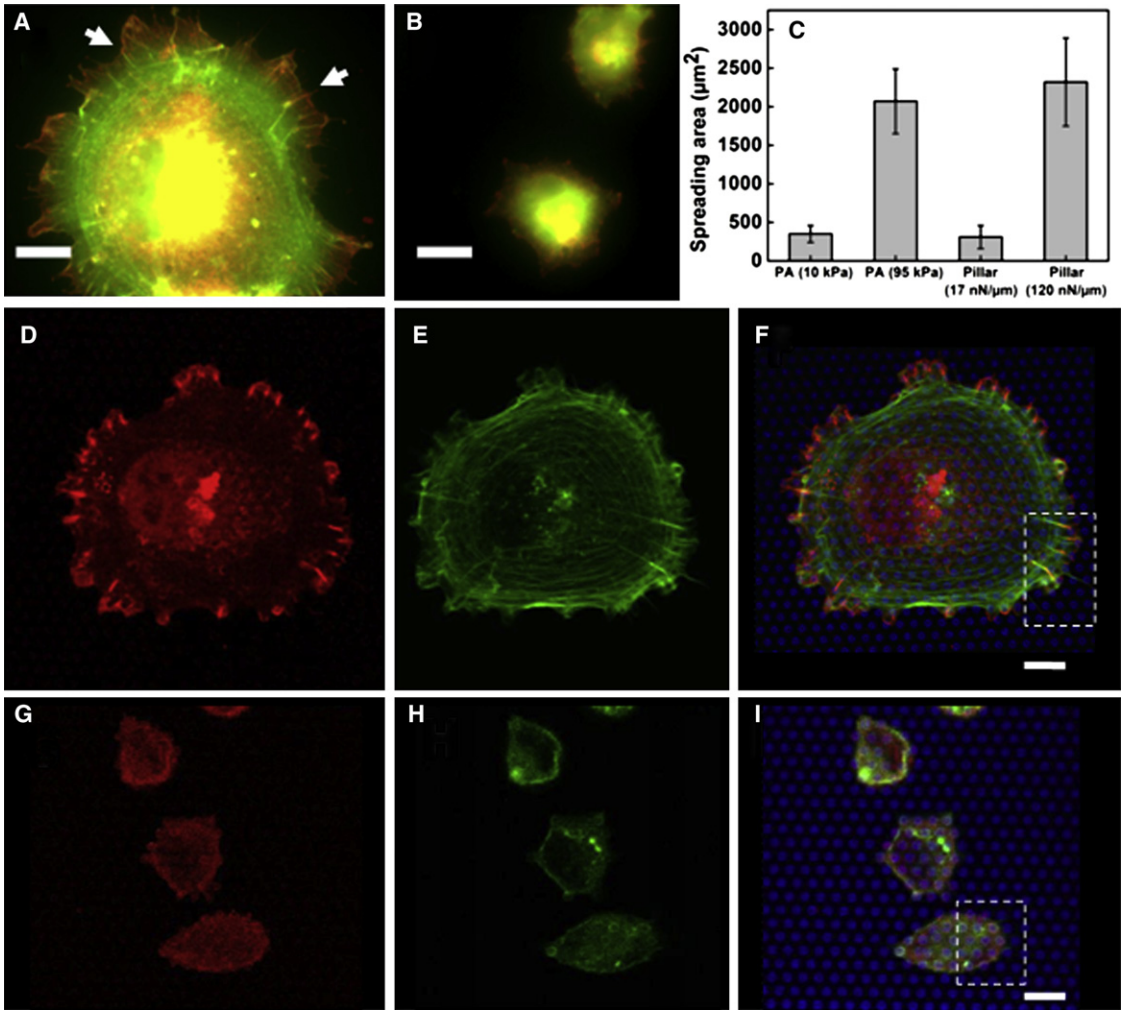

FIGURE 1 Immunofluorescent staining of C2 cells on substrates with different rigidities coated with Ncad-Fc. (*A* and *B*) PA gels with $E = 95$ and 10 kPa, respectively; Arrows in *A* indicate the location of some cadherin adhesions. Immunostaining for β-catenin (*red*), F-actin (*green*), and pillars (*blue*) was performed on cells spread on Ncad-Fc-coated pillars of two different rigidities ($k = 120$ for *D–F*, and 17 nN/μm for *G–I*) and analyzed by confocal microscopy. Scale bars: 10 μm. (*C*) Histograms of the projected spreading area of C2 cells on substrates with different stiffnesses; continuous PA gels of 10 and 95 kPa, and micropillars of 17 and 120 nN/μm.

(Fig. 2 *B*). Altogether, these results show that the assembly of cadherin adhesions could be controlled locally by the mechanical environment of the cells imposing the level of cellular tension.

Physical forces transmitted through cadherin junctions increase with the substrate rigidity

We then sought to determine how changes in the organization of the cadherin complexes and actin cytoskeleton correlate with the physical forces transmitted through cadherin adhesions on substrates with different rigidities. To that end, we determined traction forces by analyzing the deflections of the vertical micropillars whose tops were fluorescently labeled. The deflection is directly proportional to the force in the linear regime of small deformations (41). First, we verified that cells attached to the Ncad-Fc surface through cadherin adhesions and not focal adhesion structures. To do so, we performed immunofluorescent staining for β1-integrin and phospho-focal adhesion kinase (phospho-FAK), which are specific markers of focal adhesions, on C2 cells spread on stiff micropillar substrates ($k = 120$ nN/μm) coated with Ncad or fibronectin as a control (Fig. 3). These proteins were recruited in focal adhesions (Fig. 3, *B* and *D*) but not in cadherin adhesions (Fig. 3, *A* and *C*), indicating that force measurements were characteristic of cadherin-cadherin contacts.

We then performed videomicroscopy experiments to measure the forces exerted by the cells on micropillar substrates. Images were captured 2–3 h after the cells were plated on the substrates, and over time periods of 30 min. The forces detected for all of the pillars underlying the cells were collected individually (43). The mean value of the forces, $<F>$, was then plotted as a function of substrate

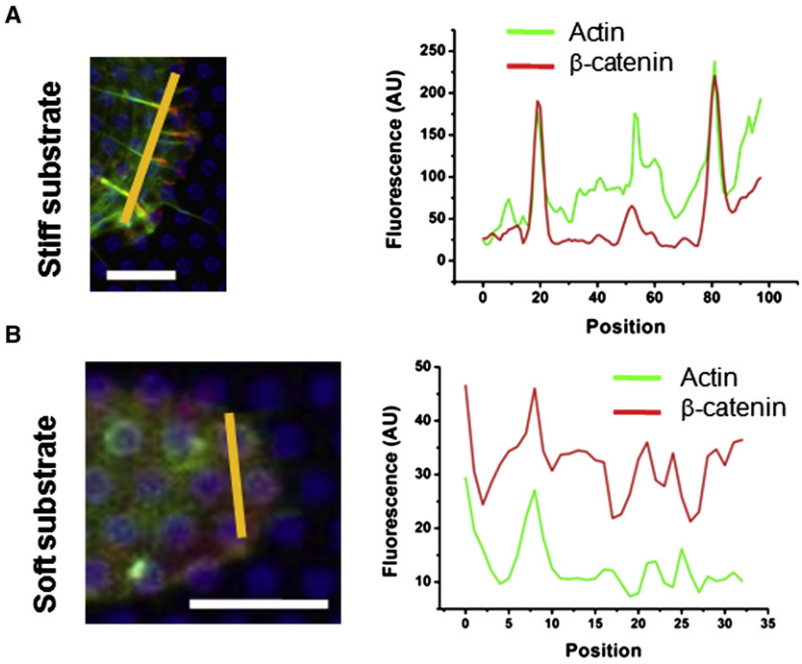

FIGURE 2 Organization of cadherin adhesions on substrates with various stiffnesses and traction forces. (*A* and *B*) Colocalization and intensity fluctuations of β-catenin (*red*) and F-actin (*green*) were analyzed along the orange line indicated on the overlay image by line scan (ImageJ software) on stiff (120 nN/μm) and soft (17 nN/μm) substrates, respectively. The images in *A* and *B* correspond to the dashed rectangles represented in Fig. 1, *F* and *I*, respectively. Scale bar = 10 μm.

rigidity. As previously observed for cells plated on substrates coated with ECM proteins (8), the average force per pillar exerted through cadherin adhesions increased from 1.6 ± 0.2 to 12.5 ± 1.3 nN, with the rigidity of the substrate in the range of 8–140 nN/μm to reach a saturation (at ~12 nN) above 140 nN/μm (Fig. 4 *A*). Again, to rule out integrin-mediated mechanosensing, we measured the average force generated per post over time for a cell cultured on Ncad-coated micropillar substrates after the addition of soluble RGD peptides (0.5 mg/mL) in the medium. It appeared that the force remained constant over time (Fig. 3 *E*).

The strengthening of cadherin adhesions was correlated with an increase of the traction forces. The saturation could be attributed to the finite size of cadherin adhesions. This approach, which mimics cell-cell contacts thanks to the flexible substrate, clearly shows that cadherin complex recruitment is modulated by local changes in the environment and mechanically alters the distribution of tensions across cells. By measuring the size of β-catenin-rich patches on stiff substrates (e.g., 120 nN/μm in Fig. 1 *F*), we obtained an average value of cadherin adhesion size of ~3.9 ± 1.3 μm^2 (Fig. 4 *B*). For a 120 nN/μm spring constant, the force was on average 12 nN with maximal values ~14 nN (Fig. 4 *A*). The corresponding stress given by the ratio of the force (~12 nN) on the average area of cadherin adhesions was found to be ~3.1 nN/μm^2. However, since we mostly measured cadherin adhesion size at the periphery of the cells, where the highest traction forces were observed, we can assume that the maximal force rather than the average one should be taken into account to evaluate the stress, which leads to a value of 3.6 nN/μm^2. This value is similar to that previously measured in focal adhesions of fibroblasts, ~5.5 nN/μm^2 (4). As in the latter case, our results indicate that mechanotransduction at cadherin adhesions probably depends on the development of stresses generated by a balance of tensile and contractile forces, presumably induced by a reinforcement of the actin cytoskeleton as shown in Fig. 1 (see Fig. 6 for a schematic model).

Actin cytoskeleton assembly and myosin II activity are necessary to sustain traction forces exerted through cadherin junctions

The mechanism by which cells modify their internal tension should involve modulation of the actomyosin contractility and in particular nonmuscle myosin II (NMM-II). NMM-II has been shown to be an important regulator of cell-cell junction formation (47), but little is known about its role in force transmission and generation at cadherin junctions. To further explore the role of myosin II in cadherin-mediated traction forces, we applied blebbistatin, an inhibitor of NMM-II, at a concentration of 50 μM on C2 cells plated on Ncad-coated substrates and analyzed the consequences on the forces. NMM-II inhibition resulted in a reduction of the force-rigidity slope over a wide range of explored rigidities (Fig. 4 *A*). An important reduction of forces (~50%) was observed, except in softer pillars (<20 nN/μm), where the reduction remained nonsignificant (<10% and smaller than the standard deviation; Fig. 4 *A*). We compared these results with those obtained from C2 cells cultured on fibronectin-coated pillars with an 89 nN/μm spring constant. Our measurements led to average forces of 15.2 ± 1.9 nN under standard conditions and 3.1 ± 1.3 nN

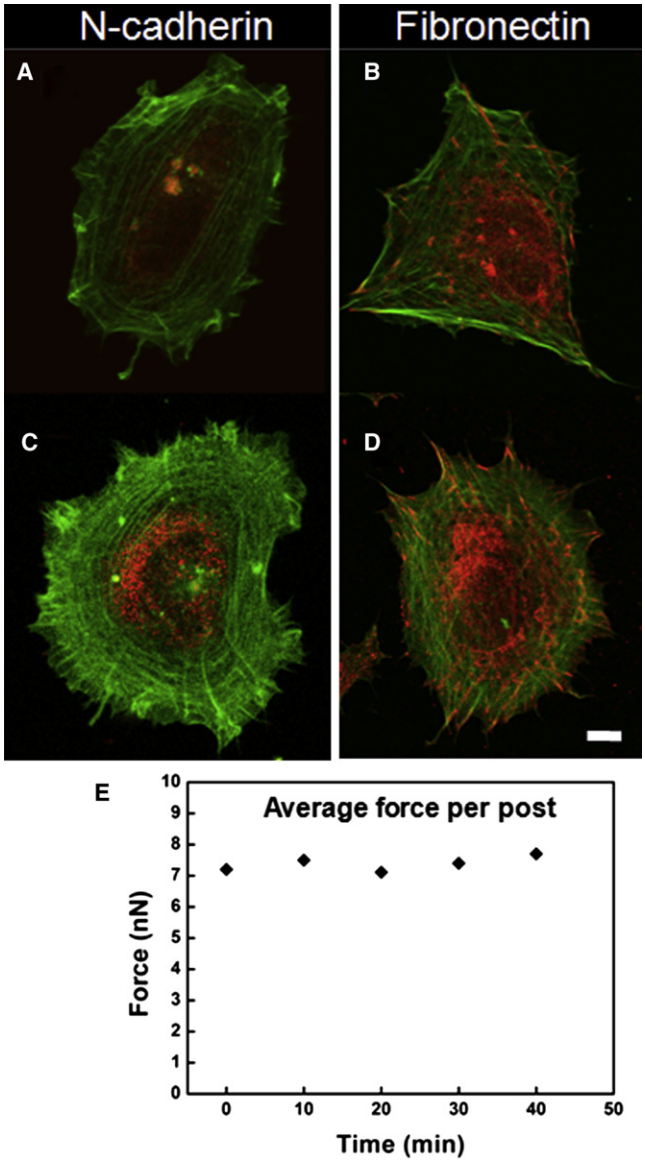

FIGURE 3 Control experiments of cell spreading on substrates coated with either Ncad or fibronectin. C2 cell spread on Ncad (*A* and *C*) and fibronectin (*B* and *D*) coated substrates were doubly stained for β1-integrin (*red*) and F-actin (*green*) or doubly stained for phospho-FAK (*red*) and F-actin (*green*). Scale bar = 10 μm. (*E*) Plot of average force generated per post over time for a cell cultured on Ncad-coated micropillar substrates (73 nN/μm) after the addition of soluble RGD peptides (1 mM) in the medium at $T = 0$.

for blebbistatin-treated cells (Fig. 4 *A*). This corresponds to an 80% decrease in the forces exerted through integrin-mediated adhesions, whereas the reduction of forces under the same conditions on cadherin-coated substrates was ~50%. Cells treated with blebbistatin may have more important residual myosin activities on cadherin substrates than on fibronectin ones, due to residual activity of NMM-II and/or other myosins. Finally, we disrupted the actin cytoskeleton of C2 cells on Ncad-coated pillars with 2 μg/mL cytochalasin D. In this case, the actomyosin network was fully disorganized (data not shown) and the traction forces were down to 0.6 and 3.5 nN for 17.2 and 120 nN/μm, respectively.

Altogether, our results suggest that the cells likely retained a residual myosin-like activity after blebbistatin treatment. Of interest, another unconventional myosin, myosin VI, has been shown to be involved in the formation of cadherin cell-cell contacts in epithelial cells (48). Nevertheless, our results demonstrate that NMM-II activity is the major molecular motor acting on the force-generation mechanism through cell-cell contacts, as well as on cadherin adhesion formation. Indeed, the labeling of F-actin and β-catenin of cells after blebbistatin treatment on a stiff substrate (120 nN/μm) confirmed that both the radial distribution of β-catenin and the distribution of actin fibers were strongly altered (Fig. 5, *A* and *B*).

Our results reveal a strong correlation between the increase of contractile forces through cadherin adhesions and cell spreading supported by the formation of actin cables and NMM-II contribution. Cells on soft substrates cannot generate sufficient traction forces via the actin cytoskeleton or promote maturation of adhesive complexes, as evidenced by the insignificant contribution of NMM-II to traction forces on softer substrates. By contrast, in a stiff environment, NMM-II is probably involved in tensioning actin structures. The well-defined actin structures are linked to well-developed adhesion plaques that ensure the transmission of forces. Indeed, previous studies have shown that NMM-II plays a key role in the recruitment of cadherin-catenin complexes and actin cables in cadherin adhesions (47,49). NMM-II is commonly believed to be involved in generating actin bundles, consistent with its role as an actin-based motor. It is therefore tempting to postulate that NMM-II-based contractility may support the formation of large cadherin clusters by bundling associated actin filaments, in a manner analogous to the mechanism by which actin stress fibers may support integrin-based focal adhesions (50).

Model of cadherin contact formation and strengthening in response to mechanical changes in cell-cell contacts

In this work, we performed experiments under various well-defined conditions to study the formation of cadherin-cadherin junctions as a function of cellular tension. The obtained results are in favor of a global rearrangement of actomyosin filaments and cadherin complexes themselves that regulate the forces transmitted through cadherin-cadherin junctions. This mechanical regulation through cadherin adhesions exhibits strong similarities with cell-to-substrate interactions through ECM proteins. The correlation between the formation of cadherin adhesions and the generated forces may be explained by a positive feedback: an increase of the force requires a reorganization of the actomyosin complexes,

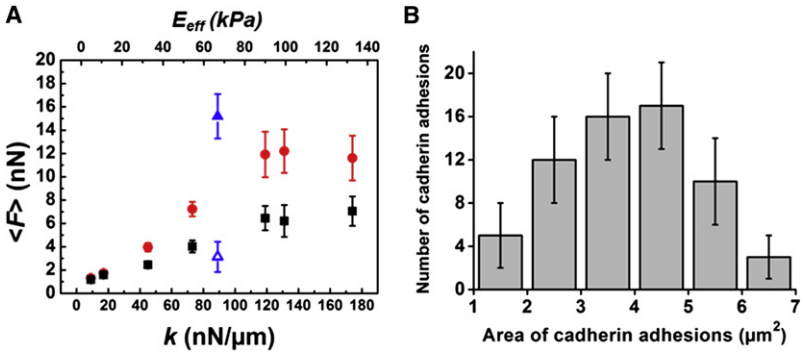

FIGURE 4 (*A*) Average forces, $<F>$, exerted by C2 cells though cadherin adhesions on micropillars as a function of substrate rigidity, k (*bottom axis*), and E_{eff} (*top axis*). The • and ■ symbols correspond to the standard conditions and the cell response after blebbistatin treatment, respectively; ~10 cells were analyzed for each rigidity. The ▲ and Δ symbols correspond to the forces exerted by C2 cells through integrin-mediated adhesions on fibronectin-coated micropillars ($k = 89$ nN/μm) without and with blebbistatin treatment, respectively ($n = 5$). (*B*) Distribution of the areas of cadherin adhesions analyzed by measuring β-catenin structures on a micropillar substrate (120 nN/μm) coated with Ncad ($n = 62$).

which in turn stabilizes the cadherin adhesions and leads to the recruitment of additional actin fibers (Fig. 6).

Although at this time we cannot propose a precise molecular mechanism for this regulation, we can suggest two molecular players: 1), myosin II itself, which has been shown to be activated via myosin light-chain phosphorylation upon E-cadherin engagement (47); and 2), members of the cadherin-catenin complex, which may undergo local molecular deformations in response to the applied tension. The latter was recently observed for talin at focal adhesions, which have been shown to unfold in response to tension, resulting in the unmasking of cryptic sites of interaction with vinculin (51). α-Catenin, which is a complex adaptor protein with multiple binding sites, is a good candidate for performing such a tension-dependent conformational change. Of interest, this protein has been shown to modulate strengthening of individual E-cadherin bonds in the range of hundreds of milliseconds after the initial engagement of a single cadherin molecule by increasing the probability of formation of additional bonds (33). Conversely, on longer timescales, α-catenin has also been proposed to mediate a switch that couples cadherin-catenin complexes to alternative actin networks of different dynamics during cell-cell contact maturation (37).

CONCLUSION

Together, these results indicate that the strength of cadherin adhesions depends not only on myosin II-dependent intrinsic tension, but also on the stiffness of the environment, suggesting that cadherin adhesions possess some kind of mechanosensor to adapt their strength to the rigidity of the intra- and extracellular environments. This adaptation likely relies on the degree of recruitment or oligomerization of cadherins in the membrane, and their association with contractile actomyosin fibers in adhesion plaques. Finally, this force-sensing mechanism of cadherins is consistent with recent findings on the connections between cadherins and fibronectin matrix observed during embryogenesis (52). The remodeling of cell junctions to exert the appropriate forces could also be particularly relevant for the maintenance of tissue integrity and the development of tumor metastasis.

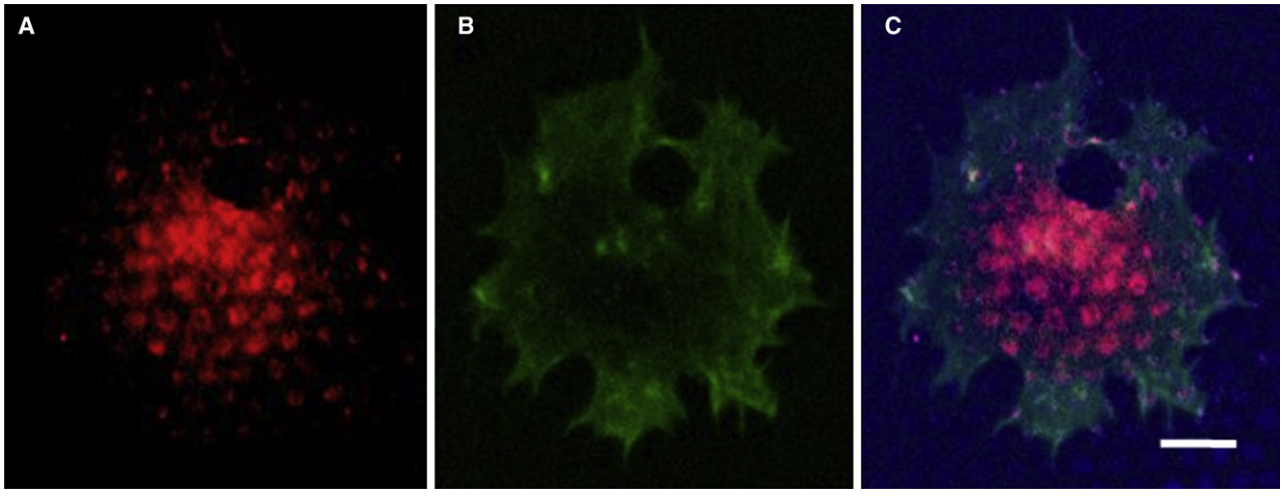

FIGURE 5 Inhibition of NMM-II affects cadherin adhesion formation and actin cytoskeleton organization. (*A–C*) Blebbistatin-treated C2 cells on a micropillar substrate coated with Ncad-Fc did not exhibit organized β-catenin radial structures. Immunostaining for β-catenin (*red*), F-actin (*green*), and pillars (*blue*) was performed on cells spread on a Ncad-Fc-coated pillar (120 nN/μm) and analyzed by confocal microscopy (optical slice focused on the top of the pillars). Scale bar = 10 μm.

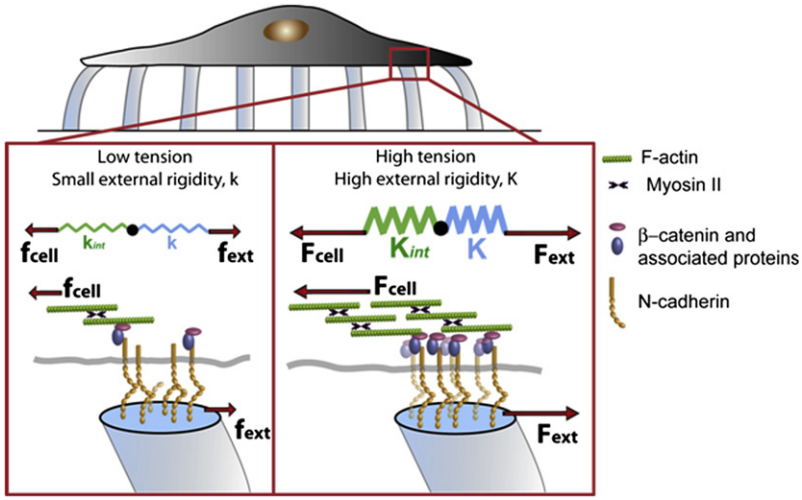

FIGURE 6 Model of cadherin contact formation and strengthening in response to mechanical changes in the cell-cell contacts. The micropillar substrate coated with Ncad represents a neighboring cell. The close-ups of cadherin contacts show the balance of external and internal forces (F_{ext} and F_{cell}, respectively). As the cell pulls on the substrate via cadherin adhesions, it induces an increase of its internal tension through the recruitment of adhesion proteins and a buildup of actomyosin contractility. On a stiff substrate (large K), the internal tension (K_{int}) is supported by the formation of large clusters of cadherin complexes aligned along actin cables. Myosin II may contribute to the contraction of actin bundles, thus promoting cadherin adhesion stabilization and reinforcement. In contrast, if the cellular environment provides less resistance to deformation when the cells pull on it (here, soft substrates with small k), small forces are observed involving a limited number of cadherin links and thus a smaller internal rigidity (k_{int}).

The authors thank R. H. Austin, A. Bershadsky, N. Biais, A. Saez, M. P. Sheetz, and Y.-L. Wang for fruitful discussions, and A. Richert for help with the cell culture protocols.

This work was supported by the Agence Nationale de la Recherche (Program PNANO 2005), the Ligue Nationale contre le Cancer (Comité Ile-de-France), the Association Française contre les Myopathies, the Comité National de la Recherche Scientifique (Interface Physique, Biologie et Chimie: Soutien à la Prise de Risque), the program C'Nano (Région Ile-de-France), and the Association pour la Recherche sur le Cancer. A.R. received postdoctoral grants from the Agence Nationale de la Recherche.

REFERENCES

1. Discher, D. E., P. Janmey, and Y. L. Wang. 2005. Tissue cells feel and respond to the stiffness of their substrate. *Science*. 310:1139–1143.
2. Keller, R., L. A. Davidson, and D. R. Shook. 2003. How we are shaped: the biomechanics of gastrulation. *Differentiation*. 71:171–205.
3. Vogel, V., and M. Sheetz. 2006. Local force and geometry sensing regulate cell functions. *Nat. Rev. Mol. Cell Biol.* 7:265–275.
4. Balaban, N. Q., U. S. Schwarz, …, B. Geiger. 2001. Force and focal adhesion assembly: a close relationship studied using elastic micropatterned substrates. *Nat. Cell Biol.* 3:466–472.
5. Munevar, S., Y. L. Wang, and M. Dembo. 2001. Traction force microscopy of migrating normal and H-ras transformed 3T3 fibroblasts. *Biophys. J.* 80:1744–1757.
6. Tan, J. L., J. Tien, …, C. S. Chen. 2003. Cells lying on a bed of microneedles: an approach to isolate mechanical force. *Proc. Natl. Acad. Sci. USA*. 100:1484–1489.
7. Galbraith, C. G., and M. P. Sheetz. 1997. A micromachined device provides a new bend on fibroblast traction forces. *Proc. Natl. Acad. Sci. USA*. 94:9114–9118.
8. Ghibaudo, M., A. Saez, …, B. Ladoux. 2008. Traction forces and rigidity sensing regulate cell functions. *Soft Matter*. 4:1836–1843.
9. Pelham, Jr., R. J., and Y. L. Wang. 1997. Cell locomotion and focal adhesions are regulated by substrate flexibility. *Proc. Natl. Acad. Sci. USA*. 94:13661–13665.
10. Riveline, D., E. Zamir, …, A. D. Bershadsky. 2001. Focal contacts as mechanosensors: externally applied local mechanical force induces growth of focal contacts by an mDia1-dependent and ROCK-independent mechanism. *J. Cell Biol.* 153:1175–1186.
11. Choquet, D., D. P. Felsenfeld, and M. P. Sheetz. 1997. Extracellular matrix rigidity causes strengthening of integrin-cytoskeleton linkages. *Cell*. 88:39–48.
12. Lo, C. M., H. B. Wang, …, Y. L. Wang. 2000. Cell movement is guided by the rigidity of the substrate. *Biophys. J.* 79:144–152.
13. Engler, A. J., S. Sen, …, D. E. Discher. 2006. Matrix elasticity directs stem cell lineage specification. *Cell*. 126:677–689.
14. Saez, A., M. Ghibaudo, …, B. Ladoux. 2007. Rigidity-driven growth and migration of epithelial cells on microstructured anisotropic substrates. *Proc. Natl. Acad. Sci. USA*. 104:8281–8286.
15. Lecuit, T. 2005. Adhesion remodeling underlying tissue morphogenesis. *Trends Cell Biol.* 15:34–42.
16. García-Castro, M. I., E. Vielmetter, and M. Bronner-Fraser. 2000. N-cadherin, a cell adhesion molecule involved in establishment of embryonic left-right asymmetry. *Science*. 288:1047–1051.
17. Gumbiner, B. M. 2005. Regulation of cadherin-mediated adhesion in morphogenesis. *Nat. Rev. Mol. Cell Biol.* 6:622–634.
18. Shen, J., C. Behrens, …, R. Lotan. 2006. Identification and validation of differences in protein levels in normal, premalignant, and malignant lung cells and tissues using high-throughput Western array and immunohistochemistry. *Cancer Res.* 66:11194–11206.
19. Dirix, L. Y., P. Van Dam, …, P. B. Vermeulen. 2006. Inflammatory breast cancer: current understanding. *Curr. Opin. Oncol.* 18:563–571.
20. de Rooij, J., A. Kerstens, …, C. M. Waterman-Storer. 2005. Integrin-dependent actomyosin contraction regulates epithelial cell scattering. *J. Cell Biol.* 171:153–164.
21. Luscinskas, F. W., S. Ma, …, S. K. Shaw. 2002. Leukocyte transendothelial migration: a junctional affair. *Semin. Immunol.* 14:105–113.
22. Rabodzey, A., P. Alcaide, …, B. Ladoux. 2008. Mechanical forces induced by the transendothelial migration of human neutrophils. *Biophys. J.* 95:1428–1438.
23. Puch, S., S. Armeanu, …, G. Klein. 2001. N-cadherin is developmentally regulated and functionally involved in early hematopoietic cell differentiation. *J. Cell Sci.* 114:1567–1577.
24. Chen, C. S. 2008. Mechanotransduction - a field pulling together? *J. Cell Sci.* 121:3285–3292.
25. Pierres, A., H. Feracci, …, P. Bongrand. 1998. Experimental study of the interaction range and association rate of surface-attached cadherin 11. *Proc. Natl. Acad. Sci. USA*. 95:9256–9261.
26. Baumgartner, W., P. Hinterdorfer, …, D. Drenckhahn. 2000. Cadherin interaction probed by atomic force microscopy. *Proc. Natl. Acad. Sci. USA*. 97:4005–4010.
27. Leckband, D., and A. Prakasam. 2006. Mechanism and dynamics of cadherin adhesion. *Annu. Rev. Biomed. Eng.* 8:259–287.
28. Prakasam, A. K., V. Maruthamuthu, and D. E. Leckband. 2006. Similarities between heterophilic and homophilic cadherin adhesion. *Proc. Natl. Acad. Sci. USA*. 103:15434–15439.

29. Perret, E., A. Leung, …, E. Evans. 2004. Trans-bonded pairs of E-cadherin exhibit a remarkable hierarchy of mechanical strengths. *Proc. Natl. Acad. Sci. USA.* 101:16472–16477.

30. Pittet, P., K. M. Lee, …, B. Hinz. 2008. Fibrogenic fibroblasts increase intercellular adhesion strength by reinforcing individual OB-cadherin bonds. *J. Cell Sci.* 121:877–886.

31. Bershadsky, A. 2004. Magic touch: how does cell-cell adhesion trigger actin assembly? *Trends Cell Biol.* 14:589–593.

32. Chu, Y. S., W. A. Thomas, …, S. Dufour. 2004. Force measurements in E-cadherin-mediated cell doublets reveal rapid adhesion strengthened by actin cytoskeleton remodeling through Rac and Cdc42. *J. Cell Biol.* 167:1183–1194.

33. Bajpai, S., J. Correia, …, D. Wirtz. 2008. alpha-Catenin mediates initial E-cadherin-dependent cell-cell recognition and subsequent bond strengthening. *Proc. Natl. Acad. Sci. USA.* 105:18331–18336.

34. Bajpai, S., Y. F. Feng, …, D. Wirtz. 2009. Loss of alpha-catenin decreases the strength of single E-cadherin bonds between human cancer cells. *J. Biol. Chem.* 284:18252–18259.

35. Adams, C. L., and W. J. Nelson. 1998. Cytomechanics of cadherin-mediated cell-cell adhesion. *Curr. Opin. Cell Biol.* 10:572–577.

36. Lambert, M., D. Choquet, and R. M. Mège. 2002. Dynamics of ligand-induced, Rac1-dependent anchoring of cadherins to the actin cytoskeleton. *J. Cell Biol.* 157:469–479.

37. Drees, F., S. Pokutta, …, W. I. Weis. 2005. Alpha-catenin is a molecular switch that binds E-cadherin-beta-catenin and regulates actin-filament assembly. *Cell.* 123:903–915.

38. Delanoë-Ayari, H., R. Al Kurdi, …, D. Riveline. 2004. Membrane and acto-myosin tension promote clustering of adhesion proteins. *Proc. Natl. Acad. Sci. USA.* 101:2229–2234.

39. Brevier, J., M. Vallade, and D. Riveline. 2007. Force-extension relationship of cell-cell contacts. *Phys. Rev. Lett.* 98:268101.

40. Lambert, M., F. Padilla, and R. M. Mège. 2000. Immobilized dimers of N-cadherin-Fc chimera mimic cadherin-mediated cell contact formation: contribution of both outside-in and inside-out signals. *J. Cell Sci.* 113:2207–2219.

41. du Roure, O., A. Saez, …, B. Ladoux. 2005. Force mapping in epithelial cell migration. *Proc. Natl. Acad. Sci. USA.* 102:2390–2395.

42. Biais, N., B. Ladoux, …, M. Sheetz. 2008. Cooperative retraction of bundled type IV pili enables nanonewton force generation. *PLoS Biol.* 6:e87.

43. Ganz, A., M. Lambert, …, B. Ladoux. 2006. Traction forces exerted through N-cadherin contacts. *Biol. Cell.* 98:721–730.

44. Gallet, F., D. Arcizet, …, A. Richert. 2009. Power spectrum of out-of-equilibrium forces in living cells: amplitude and frequency dependence. *Soft Matter.* 5:2947–2953.

45. Gavard, J., M. Lambert, …, R. M. Mège. 2004. Lamellipodium extension and cadherin adhesion: two cell responses to cadherin activation relying on distinct signalling pathways. *J. Cell Sci.* 117:257–270.

46. Solon, J., I. Levental, …, P. A. Janmey. 2007. Fibroblast adaptation and stiffness matching to soft elastic substrates. *Biophys. J.* 93:4453–4461.

47. Shewan, A. M., M. Maddugoda, …, A. S. Yap. 2005. Myosin 2 is a key Rho kinase target necessary for the local concentration of E-cadherin at cell-cell contacts. *Mol. Biol. Cell.* 16:4531–4542.

48. Maddugoda, M. P., M. S. Crampton, …, A. S. Yap. 2007. Myosin VI and vinculin cooperate during the morphogenesis of cadherin cell cell contacts in mammalian epithelial cells. *J. Cell Biol.* 178:529–540.

49. Lambert, M., O. Thoumine, …, R. M. Mège. 2007. Nucleation and growth of cadherin adhesions. *Exp. Cell Res.* 313:4025–4040.

50. Bershadsky, A., M. Kozlov, and B. Geiger. 2006. Adhesion-mediated mechanosensitivity: a time to experiment, and a time to theorize. *Curr. Opin. Cell Biol.* 18:472–481.

51. del Rio, A., R. Perez-Jimenez, …, M. P. Sheetz. 2009. Stretching single talin rod molecules activates vinculin binding. *Science.* 323:638–641.

52. Dzamba, B. J., K. R. Jakab, …, D. W. DeSimone. 2009. Cadherin adhesion, tissue tension, and noncanonical Wnt signaling regulate fibronectin matrix organization. *Dev. Cell.* 16:421–432.